Continental Shelf Research 267 (2023) 105113

Contents lists available at ScienceDirect

Continental Shelf Research

journal homepage: www.elsevier.com/locate/csr

High resolution analysis of plankton distributions at the Middle Atlantic Bight shelf-break front

Andrew J. Hirzel [a,*,1], Philip Alatalo [b], Hilde Oliver [b], Christian M. Petitpas [c], Jefferson T. Turner [d], Weifeng (Gordon) Zhang [b], Dennis J. McGillicuddy Jr. [b]

[a] Massachusetts Institute of Technology/Woods Hole Oceanographic Institution Joint Program in Oceanography/Applied Ocean Science and Engineering, 266 Woods Hole Rd, Woods Hole, MA, 02543, USA
[b] Woods Hole Oceanographic Institution, 266 Woods Hole Rd, Woods Hole, MA, 02543, USA
[c] Massachusetts Division of Marine Fisheries, 706 South Rodney French Blvd, New Bedford, MA, USA
[d] University of Massachusetts Dartmouth, 836 S Rodney French Blvd, New Bedford, MA, USA

ARTICLE INFO

Keywords:
Chlorophyll
Eddies
Fronts
Plankton
Shelf-break
Video plankton recorder

ABSTRACT

The Middle Atlantic Bight (MAB) is a highly productive ecosystem, supporting several economically important commercial fisheries. Chlorophyll enhancement at the MAB shelf-break front has been observed only intermittently, despite several studies suggesting persistent upwelling at the front. High resolution cross-frontal transects were conducted during three two-week cruises in April 2018, May 2019, and July 2019. Mesoplankton distributions at the front were measured with a Video Plankton Recorder equipped with hydrographic and bio-optical sensors. Zooplankton were also sampled with a Multiple Opening/Closing Net and Environment Sensing System. Each of the three cruises had distinctly different frontal characteristics, with lower variability in frontal position in April 2018 and higher variability in May and July 2019, primarily due to frontal eddies and a Gulf Stream warm core ring, respectively. Eulerian means of all transect crossings within each cruise did not show mean frontal chlorophyll enhancement in April 2018 or July 2019, despite individual crossings showing chlorophyll enhancement in April 2018. Transformation of the April 2018 data into a cross-frontal coordinate system revealed a weak enhancement of chlorophyll and copepods at the front. Mean frontal chlorophyll enhancement was observed in May and was associated with enhancement in the periphery of a frontal eddy rather than the front itself. None of the planktonic categories observed were enhanced at the front in the cross-shelf mean distribution, though diatom chains and copepods were more abundant inshore of the front, particularly in May and July 2019, as well as within the center of a frontal eddy in May. The high variability of the MAB frontal region obscured the impact of ephemeral frontal enhancement in mean observations of April 2018, while frontal eddies contributed to chlorophyll enhancement in mean observations of May 2019. The influence of both argues for the necessity for 3-D models rather than idealized 2-D models to explain frontal behavior and its effects on biological responses.

1. Introduction

The Middle Atlantic Bight (MAB) ranks amongst the most productive ecosystems in the world (O'Reilly and Bush, 1984), resulting in commercial fishing that contributes substantially to the regional economy (Sherman et al., 1996). The MAB occupies a broad continental shelf in the Northwest Atlantic, stretching from Georges Bank to Cape Hatteras. Within the MAB, cold and fresh water on the shelf is separated from warm and salty water offshore by a shelf-break front. Climatological conditions of the frontal region have been described by multiple studies

Abbreviations: CTD, Conductivity-Temperature-Depth; DAVPR, Digital Auto Video Plankton Recorder; EST, Eastern Standard Time; MAB, Middle Atlantic Bight; MOCNESS, Multiple Opening/Closing Net and Environment Sensing System; NES-LTER, Northeast U.S. Shelf Long-term Ecological Research; ROIs, Regions Of Interest; SPIROPA, Shelfbreak Productivity Interdisciplinary Research Operation at the Pioneer Array; SST, Sea Surface Temperature; IFCB, Imaging FlowCytobot; UTC, Coordinated Universal Time; VIIRS, Visible Infrared Imaging Radiometer Suite.

* Corresponding author. C-MORE Hale, 1950 East West Road, Honolulu, HI, 96822, USA
E-mail address: ahirzel@hawaii.edu (A.J. Hirzel).
[1] Present Address: University of Hawai'i at Mānoa, 2500 Campus Rd, Honolulu, HI 96822.

https://doi.org/10.1016/j.csr.2023.105113
Received 14 March 2023; Received in revised form 31 August 2023; Accepted 3 September 2023
Available online 7 September 2023

(Linder and Gawarkiewicz, 1998; Loder et al., 2001; Zhang et al., 2011), all of which show that the physical, biological, and chemical attributes of the shelf-break front vary significantly in both time and space. Such variabilities may come from internal or external forcing and occur over broad and fine spatial scales. Frontal meanders may have different hydrodynamic balances between meander troughs and their successive crests (Pickart et al., 1999), which may cause localized convergence or divergence. Frontal-generated submesoscale eddies (Gawarkiewicz et al., 2001), Gulf Stream warm core rings (Ryan et al., 2001), and, in rare instances, meanders of the Gulf Stream (Gawarkiewicz et al., 2018) may interact with the shelf-break front, changing its physical and biological characteristics. The high variability within and surrounding the shelf-break front poses a unique challenge in understanding its hydrographic and ecological properties, the latter of which can be influenced by both bottom-up (i.e., nutrient supply) and top-down (i.e., grazing) controls.

Elevated chlorophyll levels have been detected at the front from remotely sensed (e.g., Ryan et al., 1999a) and *in situ* (e.g., Marra et al., 1990) observations. There are a variety of processes that can enhance chlorophyll at the front, none of which are mutually exclusive – events of chlorophyll enhancement seen at the front could result from a combination of these mechanisms. When nutrients are in abundance in the early spring, Ekman re-stratification can relieve light limitation in phytoplankton, causing short-lived enhancements of chlorophyll at the front (Oliver et al., 2022). At other times of year, when nutrients are depleted in the euphotic zone, chlorophyll enhancement can potentially result from several mechanisms of upwelling at the front relieving nutrient limitation.

One mechanism for frontal enhancement is upwelling flow associated with convergence of the inshore bottom boundary layer at the foot of the front, which then detaches from the sea floor and rises toward the surface along frontal isopycnals. Bottom boundary layer convergence and detachment have been modelled for the MAB (e.g., Gawarkiewicz and Chapman, 1992; Chapman and Lentz, 1994) and observed directly in the MAB (e.g., Houghton and Visbeck, 1998; Houghton et al., 2006). Upwelling rates are typically 10 m day^{-1} (Barth et al., 1998; Benthuysen et al., 2015; Houghton and Visbeck, 1998; Houghton et al., 2006), though some estimate vertical velocities in excess of 20 m day^{-1} (Gawarkiewicz et al., 2001; Pickart, 2000).

A second proposed mechanism is upwelling of waters from the offshore interior. From a climatologically based 2-D model, Zhang et al. (2011) showed that mean flow within the surface and bottom boundary layers is predominantly offshore, due to the influence of mean wind stress and bottom Ekman layer dynamics respectively. These offshore flows are balanced by interior onshore flow parallel to the seafloor, causing mean upward motion of offshore waters with speeds of tens of cm d^{-1} to a few m d^{-1} depending on the season (Zhang et al., 2011).

A third mechanism is driven by instabilities within the shelf-break front. Frontal meanders create mesoscale and submesoscale patches of high relative vorticity, positive or negative, on either side of the shelf-break front (Zhang and Gawarkiewicz, 2015), which can result in upwelling of tens of meters per day, similar to rates estimated for bottom boundary layer convergence.

Despite evidence for the co-occurrence of chlorophyll enhancement and upwelling at the shelf-break front, the relationship between the two is poorly understood. A 2-D model by Zhang et al. (2013) suggested that upwelling may not result in a substantial increase in chlorophyll at the front because of increased grazing by zooplankton. Alternatively, the high variability of the shelf-break front may have obscured chlorophyll enhancement in the 2-D means of the observations (Zhang et al., 2013). In an *in situ* study, Hales et al. (2009b) observed bottom boundary layer detachment without a substantial increase in chlorophyll at the front. Despite measured nutrient and light levels that should have been sufficient to enhance phytoplankton growth, there was no evidence of an increase in zooplankton grazers to account for the lack of a phytoplankton increase, making these findings difficult to reconcile with models.

The objective of this paper is to address the apparent discrepancy between bottom-up stimulation of productivity via upwelling and the lack of chlorophyll and planktonic enhancement at the shelf-break front. Our observational approach consists of repeated, high resolution surveys across the front, extending into the adjacent shelf and Slope Sea waters. These surveys will be used to measure frontal biological enhancement or lack thereof, as well as cross-frontal planktonic assemblages, in order to better understand the base of the food web of this commercially important region.

2. Materials and methods

This work was completed as a component of the Shelfbreak Productivity Interdisciplinary Research Operation at the Pioneer Array (SPIROPA) project. Our study site was a section of the MAB south of Cape Cod and Nantucket Shoals, Massachusetts. Our measurements were located along a transect (Fig. 1) near the Ocean Observatories Initiative Pioneer Mooring Array (Gawarkiewicz et al., 2018). We sampled the transect approximately every other day for the duration of three two-week cruises (*R/V Neil Armstrong* AR29, 16–28/04/2018; *NOAAS Ronald H. Brown* RB19-04, 12–25/05/2019; *R/V Thomas G Thompson* TN368, 5–18/07/2019). Transect stations were 7 km apart, with the farthest inshore and offshore stations having depths of 64 m and 1882 m, respectively. This station placement and sampling frequency covers the typical location of the front between the 100-m and 200-m isobaths (Hales et al., 2009a) and can capture the passing of frontal meanders of ~15 km amplitude and 4-day period (Gawarkiewicz et al., 2004). A total of 23 transect crossings spanning all three cruises are included in this study, consisting of 317 casts. Station sampling time of day was not identical between individual transect crossings (Supplemental Table 1). Transect crossings spanning multiple year-days are labelled herein as a year-day span (e.g., year-day 132-133).

Station profiles were measured by a Seabird SBE 911+ CTD (conductivity, temperature, and pressure) and a WetLabs FLNTURTD fluorometer (chlorophyll fluorescence) mounted upon a rosette. Seawater samples were taken at discrete depths with 24 10-L Niskin bottles mounted on the rosette. CTD fluorescence was converted into chlorophyll concentration using extracted chlorophyll *a* measurements from Niskin bottle samples (Oliver et al., 2022: chlorophyll = 0.6669 × fluorescence + 0.027). To measure nitrate, phosphate, and silicate concentrations, water samples were filtered using 0.4 μm polycarbonate filters, frozen in acid-washed polyethylene bottles, and processed in the Woods Hole Oceanographic Institution Nutrient Analytical Facility. Plankton were imaged with a Digital Auto Video Plankton Recorder (DAVPR, from SeaScan Inc.) mounted upon the CTD rosette. The DAVPR included a Seabird Electronics Inc. CTD (SBE 49 FastCat), fluorometer (FLNTURTD-4620), and synchronized video camera and xenon strobe (Davis et al., 2004). Both CTD and DAVPR measurements were averaged into 1-m depth bins. DAVPR video frame frequency and dimensions were 20 Hz and 1392 × 1040 pixels. The volume imaged was ~10 × 7 × 25 mm. Plankton were extracted from video frames as "regions of interest" (ROIs) with object identification software and were saved with a time-stamp naming convention (Davis et al., 2004; For April 2018, ROIs were extracted with stricter criteria (e.g., higher sobel threshold, higher focus kernel size) due to the presence of a *Phaeocystis pouchetii* bloom in the region (Smith et al., 2021), which caused video frames to contain an abundance of out-of-focus *P. pouchetii* colonies in the background of video frames. The stricter extraction criteria were applied for all of April 2018, which resulted in lower overall category concentrations than other cruises as relatively fewer ROIs were extracted. Trends in category distribution did not appear to change based on ROI extraction criteria when tested with less stringent criteria. ROIs were manually annotated to the highest level of taxonomic identification possible based on imagery alone. Herein we focus our analysis on the most abundant categories: diatom chains and copepods (Section 3.3).

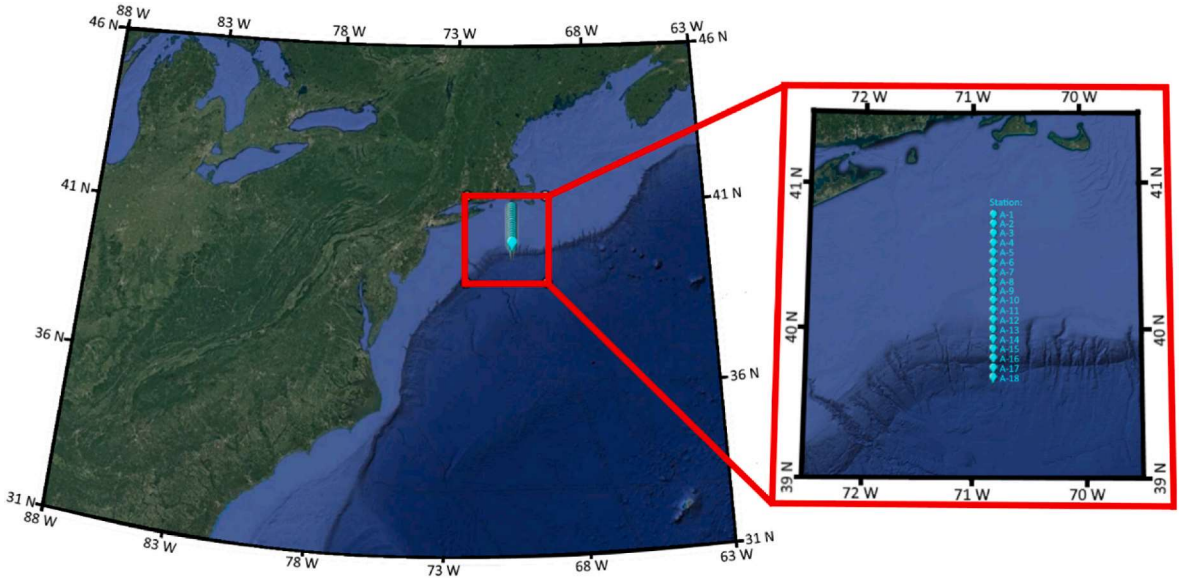

Fig. 1. General transect location, with station positions as teal markers. Station A-1 is located at 40.7 N, 70.8 W. Station A-18 is located at 39.6 N, 70.8 W. Stations are ~7 km apart along the 70.8 W meridian. The 100 m isobath is located at Station A-7. The background imagery is from Google Earth.

A 0.25 m^2 Multiple Opening/Closing Net and Environmental Sensing System (MOCNESS) (Wiebe et al., 1976) was deployed during all three cruises with a 150 μm mesh net (full methodology in Supplemental Section S.1). For reference, the typical DAVPR sampling range is 100 μm–1 cm (Davis et al., 2004), with most plankton sampled during our cruises being roughly 0.5–1 mm in length. As with the DAVPR, we focused upon copepod observations (Section 3.4). The three cruises had a total of 35 MOCNESS tows: 12 tows in April 2018, 11 tows in May 2019, and 12 tows in July 2019. With the exception of a single station sampled in late evening in May 2019, all MOCNESS tows were conducted during the day with approximately equal coverage of inshore, frontal, and offshore zones (zone criteria provided in Section 2.1).

2.1. Frontal detection and alignment

The shelf-break front is a highly dynamic region with changing hydrodynamic characteristics. For ease of comparison, we used the convention of earlier studies (e.g., Linder and Gawarkiewicz, 1998) considering the 34.5 isohaline as a metric for the location for the shelf-break front. Eulerian means were calculated from station casts by averaging measurements taken at the same station and within the same 1-m depth bins. Variability between transects was calculated by taking the standard deviation of the measurements averaged to create the Eulerian mean transects. The Eulerian mean transects for each cruise were constructed by spatially averaging 10 transect crossings (124 casts) in April 2018, 6 crossings (103 casts) in May 2019, and 7 crossings (90 casts) in July 2019 without performing frontal alignment.

For the purpose of comparison with MOCNESS tows, which were spatially and temporally sparser than DAVPR observations, we averaged MOCNESS tows by salinity. Salinities less than 34 were considered as shelf waters, salinities of more than 35 were considered as slope waters, and salinities between 34 and 35 were considered as frontal waters.

Frontal position often varied between successive transects. In such cases, computing a Eulerian mean averaged by station could smooth out and obscure patterns that might be located near the front. Previous studies have accounted for frontal movement by converting to a cross-frontal coordinate system. Cross-frontal coordinates place the position of the front as the origin, with locations onshore being negative and locations offshore being positive. Averaging under this coordinate system thus preserves relative location from the front. One major difference between the cross-frontal coordinate system used in this study and that of previous studies was that the entire vertical profile of the front was considered when converting to cross-frontal coordinates, rather than using the head (e.g., Hales et al., 2009b) or foot (e.g., Linder and Gawarkiewicz, 1998; Zhang et al., 2013) of the front. To achieve that, transect data were first bilinearly interpolated onto a horizontal grid of 1-km resolution for each 1-m depth bin. This artificial increase of the cross-shelf horizontal resolution of the station transect data from 7 km to 1 km ensured consistent resolution among all the transects. For the purpose of plotting, the location of the 34.5 isohaline at each depth was defined as the origin for each depth, such that distance from the front was determined as the original position minus the position of the 34.5 isohaline. Essentially, the frontal 34.5 isohaline was realigned vertically. This method retained the horizontal (cross-shelf) position of all data points relative to the front for all transects when averaging, regardless of the frontal structure. Matlab code for converting to a cross-frontal coordinate system is provided in Supplemental Section S.2.

3. Results

3.1. Transect Eulerian means

April 2018 had the weakest vertical stratification of the three cruises (Fig. 2). Nitrate, phosphate, and silicate were all relatively abundant throughout the water column, with the highest surface concentrations of all three cruises. Surface nitrate depletion (<0.1 μmol L^{-1}) only occurred at the farthest inshore stations above a patch of high chlorophyll (>20 mg m^{-3}). This patch originated from a regional bloom of *P. pouchetii*, with the bulk of this bloom advecting into our transect from its origin on Nantucket Shoals (Smith et al., 2021).

May 2019 had increased vertical stratification compared to April 2018. During May 2019, mid-depth chlorophyll maxima were present throughout the transect, with nitrate, phosphate, and silicate concentrations decreasing near the surface. Surface nutrient depletion was highest offshore for all three nutrients. Surface nitrate was fully depleted at stations farthest inshore of the front, cooccurring with a decline in phosphate and silicate. Surface chlorophyll was higher in May 2019 (~3.5 mg m^{-3}) than in April 2018 (~2 mg m^{-3}), excepting the *P. pouchetii* affected waters inshore in 2018. The highest chlorophyll within the May 2019 Eulerian mean was located just inshore of the shelf-break front (4.4 mg m^{-3}).

July 2019 showed the greatest vertical stratification, due to the

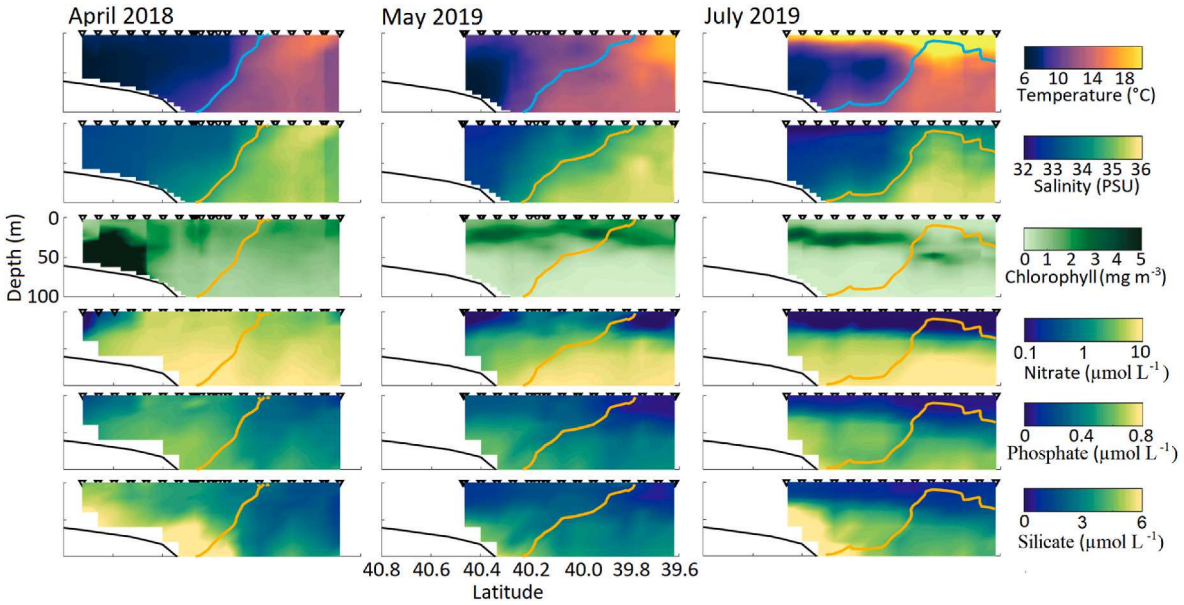

Fig. 2. Eulerian mean transects for each of the three cruises. Nitrate concentration is plotted on a nonlinear scale to highlight changes in surface concentration. The locations of the 34.5 isohaline are denoted by the teal (temperature plots) and orange lines (all other plots). Station locations are denoted by the black triangles above the transect, though not all stations were sampled for each transect. The 34.5 isohaline extends offshore in July 2019 due to a streamer caused by a Gulf Stream warm core ring. The waters most characteristic of offshore waters in this cruise are located 39.8–40° N, where the 34.5 isohaline is closest to the surface. Plots of the individual transects that were used to calculate Eulerian means are shown elsewhere (Top three rows: May 2019 – Fig. 6, April 2018 and July 2019 – Supplemental Figs. 1–2; Bottom three rows: Supplemental Figs. 6–8).

formation of a seasonal thermocline with a shallow mixed layer. Chlorophyll maxima in July 2019 were located below the warm surface mixed layer. Nitrate, phosphate, and silicate were all depleted in the surface throughout the transect, with full nitrate depletion above 30 m depth. Offshore of the front, both the warmer surface layer and the euphotic zone extended deeper, resulting in deeper chlorophyll maxima and deeper nutrient depletion.

3.2. Frontal variability in Eulerian means

Variability in cross-shelf position of the front head (surface expression) was greater than that of the front foot on the seafloor for all cruises (Fig. 3, top row). April 2018 had the least variability in frontal position overall and the sharpest gradient between shelf and Slope Sea waters, as reflected by the most vertical isohalines. Salinity variability in April 2018 (Fig. 3, middle row) had peak values in the surface layer, corresponding to the cross-shelf motion of the front head. Note that some of the variability on the offshore end resulted from the influence of a Gulf Stream warm core ring in the last few transect crossings (Supplemental Fig. 1, year-days 115 through 117–118). Chlorophyll variability in April 2018 (Fig. 3, bottom row) was primarily associated with the inshore *P. pouchetii* bloom and not with the front.

In contrast, July 2019 had the highest salinity variability and the greatest change in frontal position among the three cruises (Fig. 3, rightmost column). Salinity variability was highest south of approximately 40° N and within the upper 50 m, due to shelf water being advected offshore in a streamer associated with a Gulf Stream warm core ring for the first few transect crossings of the cruise (Fig. 4, Supplemental Fig. 2, year-days 187, 188) (Zhang et al., 2023). This streamer maintained the physical properties of shelf water in the upper 50 m of the water column, extending the offshore end of shelf waters to south of 39.5° N and out of range of our transect. After the streamer passed, the shelf-break frontal structure was restored, and the front head returned to approximately 40° N. The mean position of the foot of the front in July

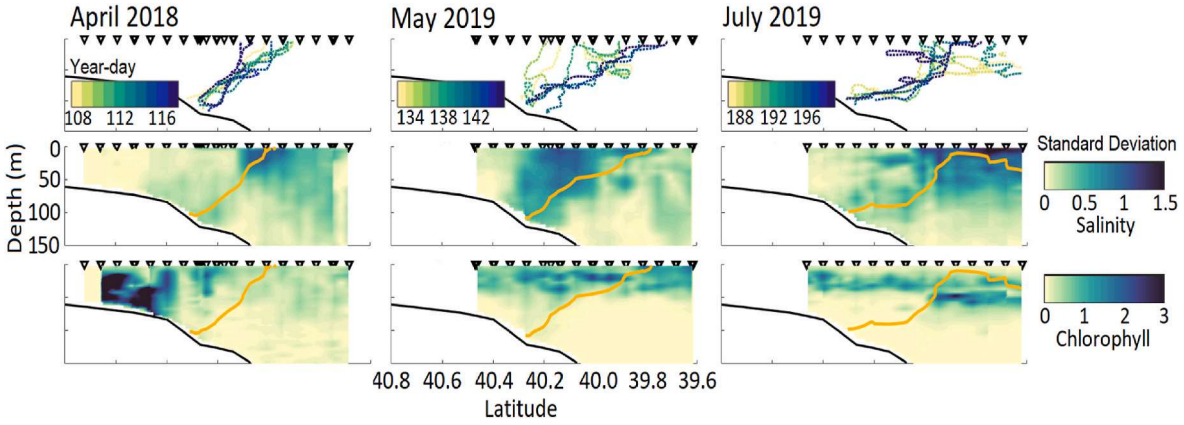

Fig. 3. Top row) location of the 34.5 isohaline for all transects used to compute mean transects for each cruise. Colors indicate transect date, with yellow being the start of each cruise. Lower two rows) standard deviation of the same values used to compute mean observations, over the same depth/distance bins, for both salinity and chlorophyll. Triangles above the means represent stations used. The orange line represents the mean location of the 34.5 isohaline for each cruise.

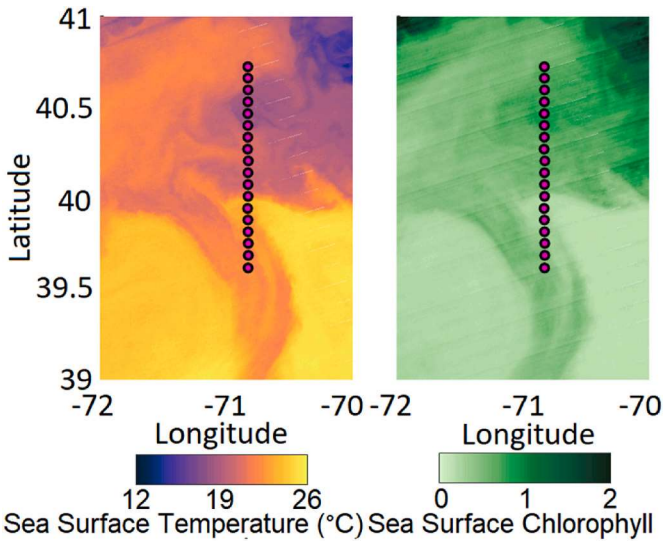

Fig. 4. Satellite snapshot of the streamer observed on year-day 191 in July 2019. To the left of the streamer is the Gulf Stream warm core ring causing the streamer. The location of the front was at approximately 40° N.

2019 was also located farthest inshore of all cruises, making the mean frontal slope the least steep in July. Chlorophyll variability was highest in waters offshore of the front at approximately 50 m (Fig. 3). This was associated with a deep chlorophyll maximum (Fig. 2) driven by a water mass intrusion of Gulf Stream origin. Described in more detail by Oliver et al. (2021), this chlorophyll enhancement was observed when high salinity (>35.6), high nutrient deep Gulf Stream water was lifted into the euphotic zone. The time-averaged imprint of this phenomenon is manifested as a chlorophyll maximum at 50 m located at 39.9°N (Fig. 2). Individual transect crossings, e.g., year-day 195, had salinities above 36 co-located with chlorophyll maxima (Supplemental Fig. 2).

Unlike both April 2018 and July 2019, May 2019 showed little salinity variability at the mean location of the head of the shelf-break front or offshore (Fig. 3). Peak salinity variability was instead inshore of the front, in waters above the foot of the front. This pattern was the result of frontal eddies that were present in all transect crossings in May 2019 (Figs. 5 and 6). The first three crossings were influenced by Eddy A (Fig. 6, first three rows) and the later three were influenced by Eddy B (Fig. 6, latter three rows).

Eddy A began as a filament of warm and salty water from the southeast, which separated cold and fresh shelf waters to the north of the slope water filament from a filament of cold and fresh waters to the south (Figs. 5 and 6). Subducted shelf waters are present at roughly 50 m

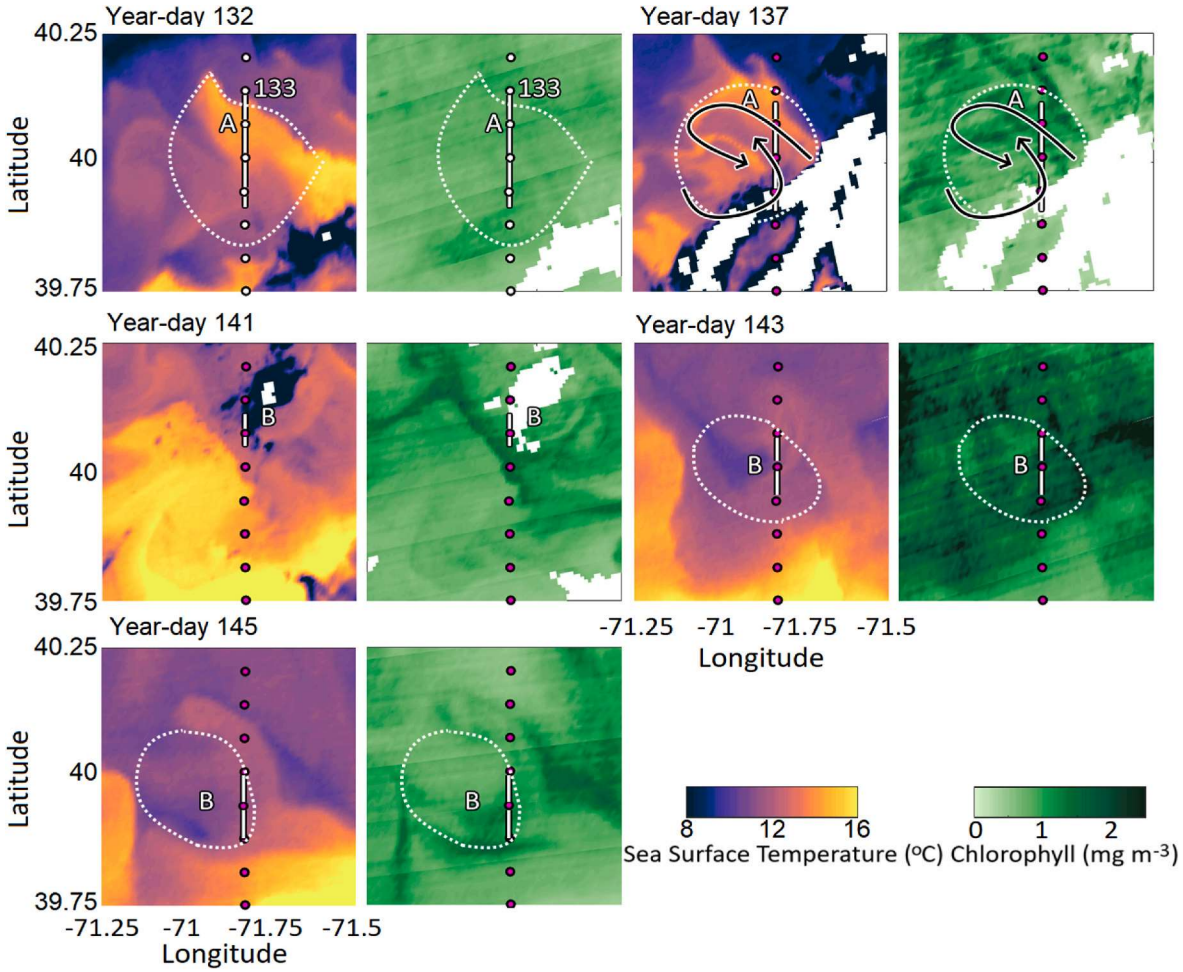

Fig. 5. Visible Infrared Imaging Radiometer Suite (VIIRS) satellite snapshots of features A and B during May 2019, along with temperature transects of each feature. Features in satellite snapshots are roughly outlined by circles and marked by letters within transect plots. The shelf-break front was located south of both features, at approximately 40° N. Station locations are marked by magenta or white dots in satellite images based on whether the transect was or was not sampled respectively on that year-day. White lines represent the location of each feature within transect plots (Fig. 6), with letters denoting each feature. White dotted lines show the approximate border of features. The transect for year-day 132-133 was used as reference for the satellite image of year-day 132. Black arrows on year-day 137 represent the slope and shelf water filaments.

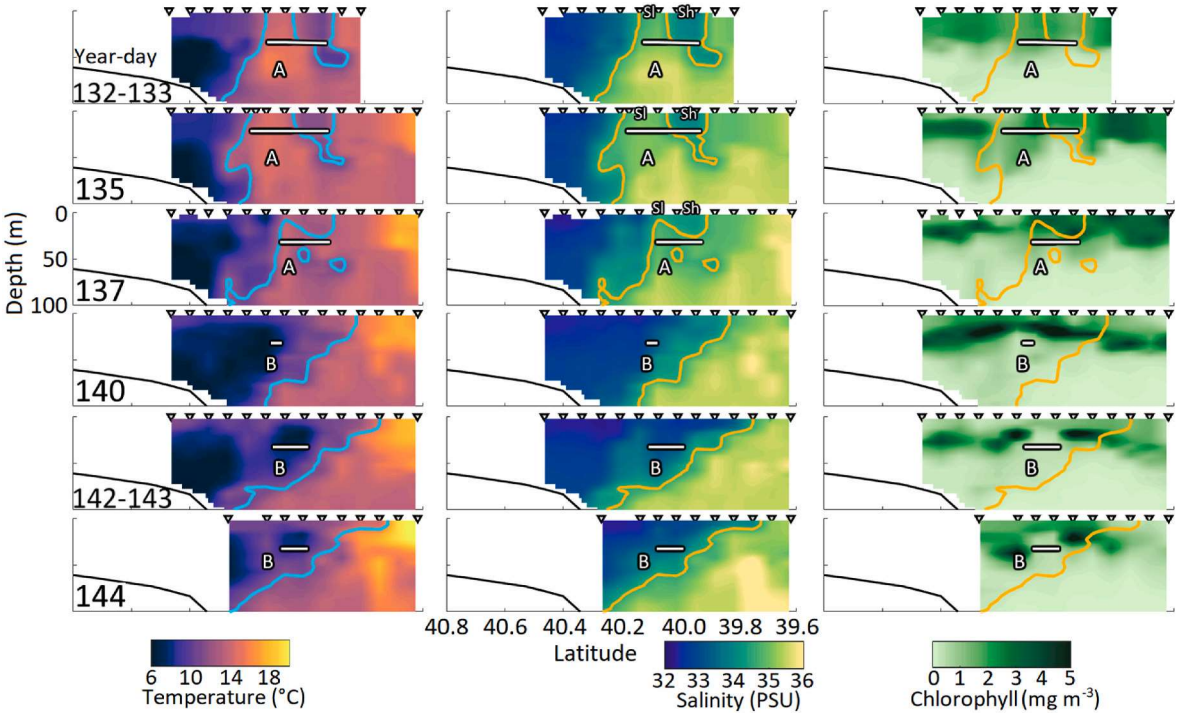

Fig. 6. All individual transects used to create Eulerian mean plots (Fig. 2) for May 2019. Stations sampled are denoted by triangles above plots. The 34.5 isohaline is represented by the teal and orange lines. Letters approximate the centers for frontal features A and B. The white lines at the bottom of each plot mark the extent of each feature within the transects. Letters denote which feature was observed during that transect. The letters "Sl" and "Sh" on salinity plots denote the slope and shelf water filaments respectively.

at the deepest point of the shelf filament, extending southwards. Surface chlorophyll in both filaments was approximately equal to background shelf chlorophyll for year-days 132-133 and 135, both in satellite imagery and *in situ* observations. By year-day 137, both filaments elongated and spiraled towards eddy center (Fig. 5 upper right). Subducted shelf waters were no longer coherent by year-day 137, with only remnants visible. Chlorophyll was enhanced in the frontal eddy relative to surrounding waters (Fig. 6, third row), although the enhancement was less evident in satellite imagery (Fig. 5, upper right). After moving off of the transect (year-day 141), Eddy A had transitioned into a frontal eddy and was no longer discernible from surrounding slope waters.

Eddy B was composed primarily of shelf water, with a core of cold, fresh cold pool water surrounded by slightly saltier and warmer waters more characteristic of shelf waters close to the front. All waters of Eddy B had salinities less than 34.5. Eddy B was characterized by a ring of chlorophyll enhancement around its periphery, which persisted for three ship-based crossings of the eddy. A thin lens of shelf water covering Eddy B (Fig. 6, last two rows) prevented precise identification of Eddy B in satellite imagery (Fig. 5, year-days 142-143 and 145), but the patterns in SST and surface chlorophyll are indicative of the eddy's presence. For example, a filament of warmer water was advected around the eastern flank of Eddy B on year-days 142-143 and 145. Surface chlorophyll was marginally higher in satellite imagery in association with both water masses around the periphery of Eddy B. No major changes in hydrographic properties or chlorophyll were evident over the duration that Eddy B was observed.

Neither eddy appeared to be unique; many such eddies occurred at and near the front during May 2019 as well as in other years. Satellite imagery for year-day 142 in particular showed several eddy-like features in close proximity to our transect line (Fig. 7). Eddies A and B are present (the same eddies as in Figs. 5 and 6), along with two additional eddies, C and D. All four eddies appear to represent similar phenomenology at varying ages with local patches of chlorophyll enhancement.

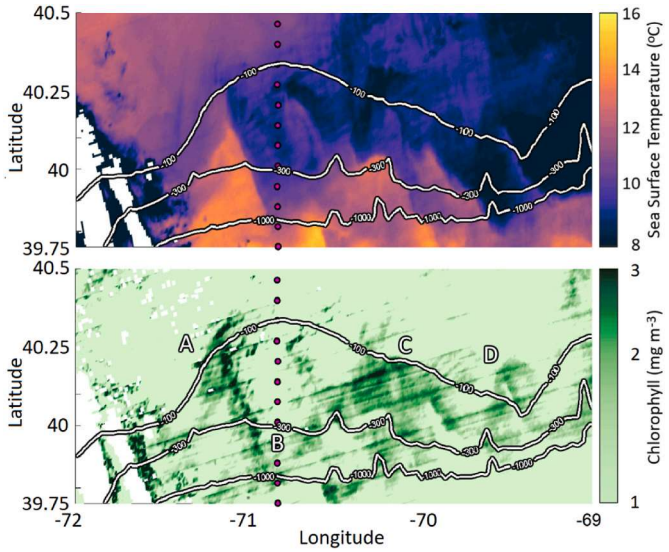

Fig. 7. VIIRS SST (top) and chlorophyll (bottom) for year-day 142. Transect stations are shown as magenta circles. Letters in the lower panel represent the approximate locations of eddies A and B, as well as two other features (C and D). White lines represent the 100, 300, and 1000 m isobaths. The foot of the front is typically near the 100 m isobath. Note the logarithmic spacing and shifted range of the chlorophyll values in the color bar to better illustrate features near the front.

3.3. Planktonic observations

ROIs from DAVPR observations were manually annotated into 31 categories, with three planktonic categories constituting over 90% of the total distribution of planktonic ROIs (Fig. 8). *P. pouchetii* comprised approximately three quarters of the total and diatom chains and

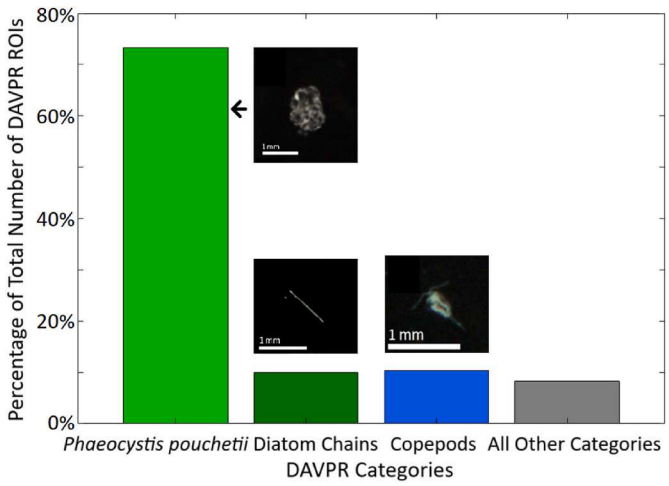

Fig. 8. The relative proportion of ROIs from all three cruises that were classified as a given category. The rightmost, gray bar contains the combined number of ROIs that were classified as other categories. ROIs displayed are sample ROIs for each of the three predominant categories.

copepods comprised 10% each. Most other individual planktonic categories typically contributed less than 1%. The high *P. pouchetii* abundance came almost entirely from April 2018, with the vast majority coming from the inshore regional bloom mentioned earlier. Since *P. pouchetii* had little presence at the front, we focused primarily on the remaining two common categories, diatom chains and copepods. Individuals of both categories were roughly the same size (approximately 1 mm).

Mean distributions of diatom chains and copepods showed complex relationships with mean hydrographic and chlorophyll distributions (Fig. 9). Chlorophyll, diatom chain, and copepod concentrations were all positively correlated with each other (Supplemental Table 2). Though statistically significant, these correlations were weak, as expected. Specifically, diatom chains comprise only a fraction of total chlorophyll and comprise only a portion of the copepod diet. Moreover, the relationships between these variables are highly dynamic and time-dependent given the strong oceanographic forcing in this regime.

Abundance of both categories was lowest in April 2018 and higher in May and July 2019, although this may reflect the stricter criteria used for ROI extraction for April 2018. Diatoms and copepods were abundant inshore in April 2018, near the *P. pouchetii* bloom. Diatom chains were also abundant offshore in April 2018 to a lesser extent. The offshore enhancement co-occurred with the slightly higher offshore mean chlorophyll concentrations compared to shelf concentrations outside the *P. pouchetii* bloom (Fig. 2). The mean distribution of diatom chains in May 2019 (Fig. 9) shared some qualitative similarities with mean chlorophyll (Fig. 2). However, the peak in diatom chains occurred one station farther inshore than that of the peak in chlorophyll, within a region of relatively lower mean chlorophyll. Small copepod abundance showed no mean enhancement at the front. Both mean diatom and small copepod abundances were highest in May 2019 at the two stations farthest inshore.

No mean enhancement in either diatoms or copepods was seen at the front in July 2019, compared to abundances farther inshore and offshore (Fig. 9). July mean diatom distributions generally corresponded with mean chlorophyll distributions, with peak diatom chain concentrations for this study (>1000 diatoms L^{-1}, Supplemental Fig. 5) observed in association with offshore Gulf Stream intrusions. Concentrations on our transect were similar in magnitude to those reported by Oliver et al. (2021) within Gulf Stream intrusions southeast of our transect. Like in May 2019, diatoms and copepods in July 2019 were both abundant in mean observations at stations farthest inshore of the front. However, in July 2019 the peak mean diatom concentrations were located below the mixed layer, co-occurring with peak mean chlorophyll, while the peak in copepods were instead located within the surface mixed layer.

The variability observed in May 2019 provided an opportunity to examine synoptic relationships between hydrography, chlorophyll, diatom, and small copepod distributions (Fig. 10). While chlorophyll on year-days 132-133 and 135 was roughly constant throughout Eddy A (Fig. 6, right column, first two rows), diatom chains and copepods were enhanced in shelf waters around the periphery of the eddy. Nutrients were present in near-surface waters within the interior of Eddy A without significant increases in chlorophyll or diatom chains. Eddy B had chlorophyll enhancement around the periphery (Fig. 6), while diatom chains and copepods were enhanced in the center of the eddy, where nutrient concentrations were elevated (Fig. 10).

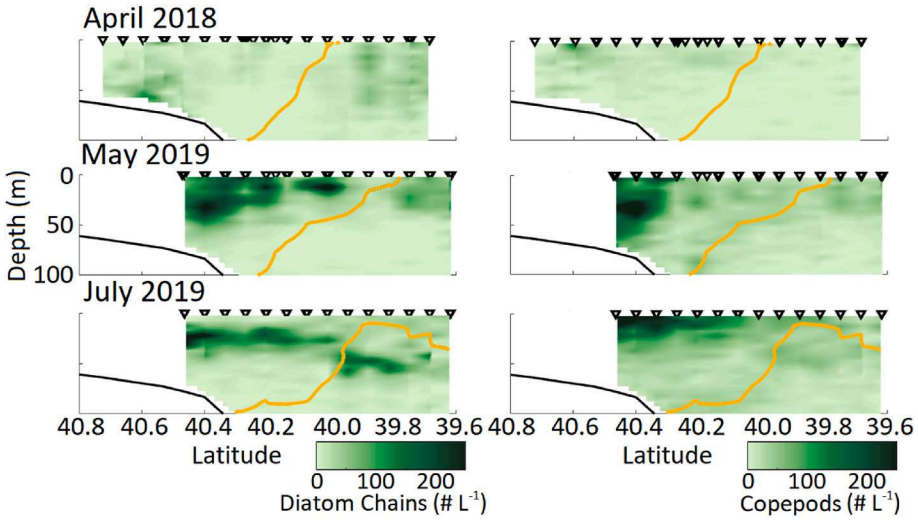

Fig. 9. Eulerian means of the diatoms and copepods for each of the three cruises. The orange line is the 34.5 isohaline. Station locations are denoted by the black triangles above the transect, though not all stations were sampled for each transect. Plots of the individual transects that were used to calculate Eulerian means are included as Supplemental Figs. 3–5.

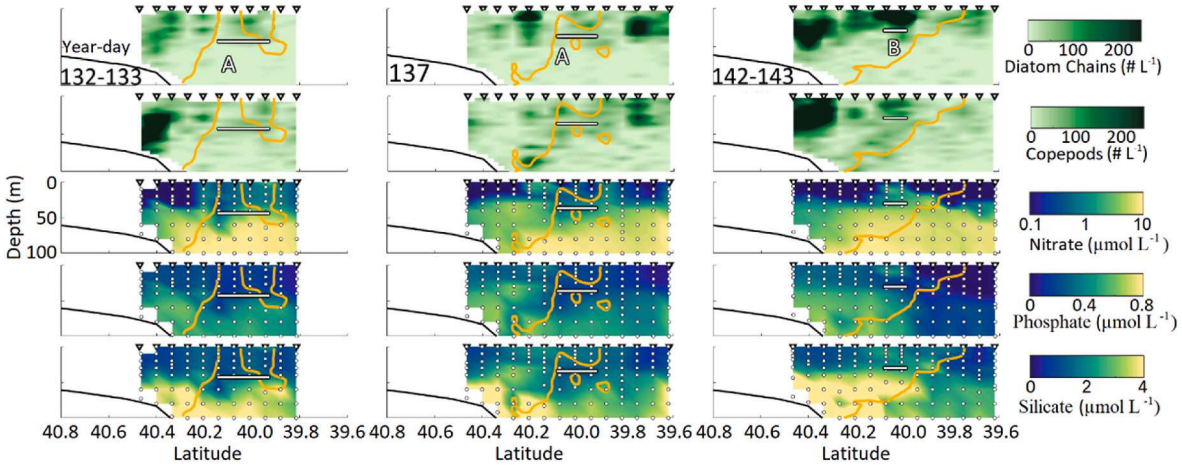

Fig. 10. Individual transects for half of the transects for May 2019. Nitrate concentration is plotted on a nonlinear scale to highlight changes in surface concentration. The orange line is the 34.5 isohaline. Station locations are denoted by the black triangles above the transect. White dots represent the depths for which nutrient bottles were sampled, with the colors on nutrient plots being the interpolated depths as calculated for constructing Eulerian mean transect plots. The white lines at the bottom of each plot mark the extent of each feature within the transects. Letters denote which feature was observed during that transect.

3.4. MOCNESS observations

Consistent with the DAVPR results, the MOCNESS data do not show evidence of mean enhancement of copepods at the front (Fig. 11). MOCNESS copepod abundances were highest in shelf waters in May 2019 and July 2019, as was the case for DAVPR measurements. In April 2018, the MOCNESS tows showed concentrations of copepods on the shelf that were lower than the front and slope, in contrast to the DAVPR measurements that showed consistently higher copepod abundance in shelf waters. The apparent discrepancy between the two sampling systems in April 2018 may have been due to the timing and locations of MOCNESS tows, which primarily sampled shelf waters outside of the dense bloom of *P. pouchetii*, where DAVPR-derived copepod concentrations were relatively high. Overall MOCNESS concentrations were lower than those of DAVPR observations, which can be at least partially attributed to differences in sampling time in addition to intrinsic instrumental differences. DAVPR observations were collected during both night and day, while MOCNESS observations were taken primarily during the day, in order to coincide with measurements of primary productivity. Time of day for MOCNESS and DAVPR sampling matters because of zooplankton diel vertical migration. Many herbivorous copepods ascend to shallow depths at night to feed on abundant phytoplankton produced by daytime photosynthesis, when predation risk from visually feeding predators is reduced by darkness. These copepods then descend during daytime in order to avoid visual predation in darker waters at depth (Bandara et al., 2021).

Comparison of chlorophyll, diatom chains, and copepods at different times of day during different transects showed no strong diel trends for any of our three cruises (Supplemental Fig. 9). Both inshore (stations A-5 to A-8) and offshore (stations A-15 to A-18) casts were predominately influenced by the various oceanographic features identified above (Section 3.2). The experimental design of this study does not provide the temporal resolution necessary to identify a diel signal through spatial variability. The lack of visible diel trends does not negate our hypothesis for differences measurements between the MOCNESS and the DAVPR, rather, these results once more emphasize the large factor that oceanographic variability plays in this region.

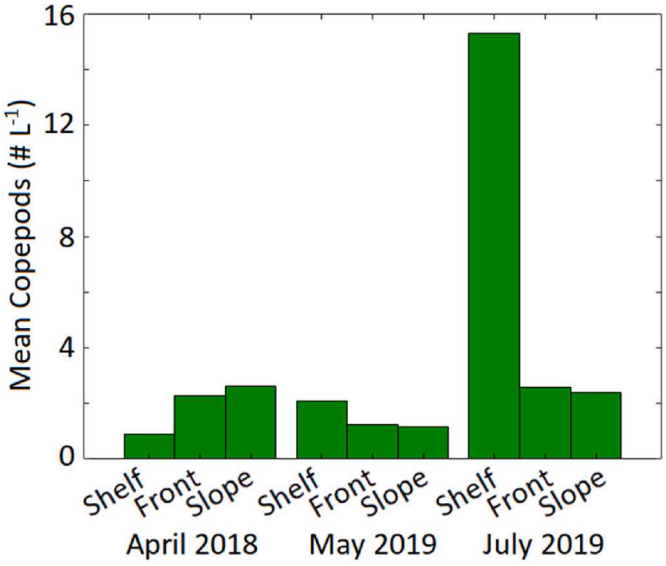

Fig. 11. Mean copepod abundances from MOCNESS tows for all three cruises. Regimes are determined by salinity, with <34 being shelf waters, >35 being slope waters, and the front in between.

3.5. Frontal alignment

Our frontal alignment methodology was designed to correct for variations in frontal position under the condition that the location of the front can be clearly and unequivocally identified with the 34.5 isohaline metric. This was possible in April 2018 due to the high horizontal stratification between inshore and offshore waters. May and July 2019 contained frequent obstructions, primarily in the form of frontal eddies and a warm core ring streamer respectively, making head-to-foot frontal alignment impractical. As mentioned previously, April 2018 individual transects contained patches of highly transient chlorophyll enhancement, which were present on either side of the front. Frontal alignment of April 2018 measurements yielded slightly higher concentrations of mean chlorophyll and copepods inshore of the front (Fig. 12). However, in neither case was this enhancement more than one standard deviation from the mean of surrounding surface waters.

4. Discussion

4.1. April 2018

Our Eulerian mean measurements found no mean chlorophyll, diatom, or small copepod enhancement at the front in April 2018 and

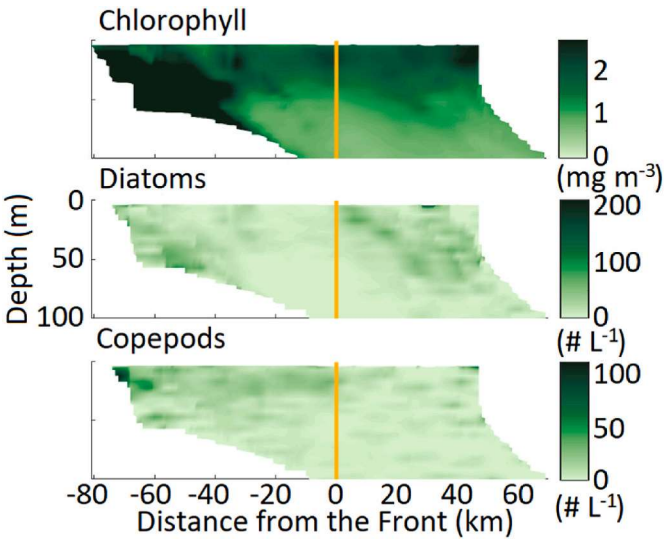

Fig. 12. Frontal alignment means for April 2018 for chlorophyll, diatoms, and copepods. The orange line represents the location of the 34.5 isohaline, which is identically zero on the horizontal axis.

July 2019. This is not a surprising conclusion for July 2019, where chlorophyll, diatoms, and copepods were primarily abundant in association with the offshore Gulf Stream intrusions or inshore, away from the front. However, several transect crossings in April 2018 showed chlorophyll enhancement at the front (Supplemental Fig. 1). For example, year-day 107-108 showed particularly strong chlorophyll enhancement as a result of wind-driven Ekman restratification (Oliver et al., 2022). Enhancement also occurred on opposites sides of the front, in close succession. Chlorophyll measurements at the front were highest in shelf waters on year-day 109 and highest in slope waters on year-day 110-111 (Supplemental Fig. 1). None of these ephemeral chlorophyll enhancements in April 2018 show up in Eulerian mean observations (Fig. 2). However, averaging with a frontally-aligned coordinate system shows enhancement of chlorophyll at the front (Fig. 12), along with copepods. Thus, in this particular case, frontal movement and variability obscured frontal enhancement in the Eulerian mean observations.

Averaging satellite chlorophyll for multiple years for the month of April in a Eulerian system shows a similar result as we observed, with minimal difference between mean shelf and frontal chlorophyll and higher chlorophyll variability at the front (Fig. 2 from Saba et al., 2015). The higher chlorophyll variability at the front implies that the transient frontal chlorophyll enhancements we observed in April 2018 may be both common and obscured by satellite observation. Implementing some form of frontal alignment, via either salinity as done here or by topography as in Oliver et al. (2022), may permit further exploration into the broader impact of these features.

Diatom chains were not abundant within the transient frontal chlorophyll enhancements observed in April 2018 (Supplemental Fig. 3). At least one ephemeral frontal chlorophyll enhancement, that of year-day 107-108, was associated with an enhancement of nanoplankton, which are too small to be imaged by the DAVPR (Oliver et al., 2022). Nitrate, phosphate, and silicate were available in surface waters at the front throughout April 2018, despite decreases in concentration inshore and offshore. This extended nutrient availability could be due to upwelling.

4.2. May 2019

May 2019 had chlorophyll enhancement at the front and this enhancement is attributed to frontal eddies. Nutrients were present in near-surface waters within the interior of both eddies, indicative of upwelling (Fig. 10). The interior of Eddy A did not contain significant increases in chlorophyll or diatom chains, perhaps because upwelling had occurred recently in the eddy core, and insufficient time had passed for the biological response. Subsequent surface chlorophyll enhancement within Eddy A on year-days 141 and 142 support this hypothesis (Figs. 5 and 7).

Eddy B had chlorophyll enhancement around its periphery (Fig. 6), while diatom chains and copepods were enhanced in the center of the eddy. This corresponded with notable increases in nitrate, phosphate, and silicate within the center of Eddy B, which is suggestive of a recent upwelling event. The coincidence of diatom chains and copepods could be indicative of a community shift as a result of grazing on smaller phytoplankton by copepods, leaving the larger diatom chains sampled by the DAVPR to flourish. Another possibility is that rapidly growing diatoms responded most quickly to the upwelled nutrients, and copepods aggregated there (perhaps through vertical migration) to graze on them. Yet another possibility is that the high concentrations of diatoms and copepods reflect the community composition of their source waters in the cold pool farther inshore. In any case, the lower chlorophyll within the center of Eddy B despite diatom chain enhancement implies that diatom chains were a small component of the total chlorophyll and/or a had a higher carbon:chlorophyll ratio than other types of phytoplankton.

Surface underway observations in May 2019 made with flow cytometry and Imaging FlowCytobot (IFCB) (see Fig. 5.12 in Archibald, 2021) documented higher total biovolume concentrations of both picoplankton and nanoplankton in front waters (defined as 34–35 salinity) compared to shelf (<34) concentrations, at the same location as we saw enhancement in mean chlorophyll (Fig. 2). Most of the subsurface chlorophyll enhancements associated with Eddy B are likely not visible in these surface observations. However, year-day 137 had surface chlorophyll enhancement at the front, as did year-day 144, though chlorophyll on that day was primarily located at depth (Fig. 6). Neither of these high chlorophyll patches were associated with high diatom chain abundance (Supplemental Fig. 4).

The overall mean enhancement of chlorophyll at the front in May 2019 was driven by chlorophyll enhancement on the periphery of Eddy B, supporting the hypothesis that frontal eddies can enhance chlorophyll at the front. As noted previously, neither of the eddies we observed were unique (Fig. 7). Previous studies have observed both similar eddies (e.g., Eddy A: Garvine et al., 1988; Eddy B: Flagg et al., 1997) and similar chlorophyll patches (e.g., May 1980, 1984 (both from Fig. 2 of Ryan et al., 1999a), and 1997 (Plate 1 of Ryan et al., 1999b)), indicating that the frontal eddies such as observed during May 2019 are common and may be important to biological communities near the front.

4.3. July 2019

July 2019 was unlike either April 2018 or May 2019 in that the observed variability was driven predominately by external forcing from a Gulf Stream warm core ring. Although offshore forcing did play some role at the end of both the April 2018 and May 2019 cruises, our main findings of transient frontal chlorophyll enhancement in April 2018 and the effects of frontal eddies in May 2019 were primarily driven by frontal behavior. In contrast, the strongest biological signals in July 2019 occurred away from the front: an enhancement of diatom chains and copepods inshore, and diatom hotspots offshore (Oliver et al., 2021). The front appears to be a local minimum in terms of chlorophyll, diatom chains, and copepods, with nearby enhancement attributable to external forcing. Nor are we alone in this finding – Hales et al. (2009b) observed a similar chlorophyll minimum at the front in August 2002, though they also observed evidence of bottom boundary layer detachment. It may be that once surface nutrients have been depleted and vertical stratification limits the supply of nutrient rich deep waters, biological communities are not enhanced at the front.

4.4. Climatological comparison

April 2018 mean frontal position and structure were most similar to winter climatological means (Zhang et al., 2011) (Fig. 3, upper left). Nutrient and chlorophyll distributions most closely matched the general pattern of winter climatological distributions (Zhang et al., 2013), in that nutrients were available throughout our transect and chlorophyll was much higher inshore. Later individual transect crossings in April 2018 (e.g., year-days 115-116, 117–118) showed nutrients and chlorophyll distributions that were more similar to spring climatological conditions (Zhang et al., 2013).

May 2019 mean frontal position and structure were most similar to spring climatological means (Zhang et al., 2011) (Fig. 3 middle column). Mean May chlorophyll and nutrient distributions (Fig. 2, top middle) were similar to climatological distributions (Zhang et al., 2013), indicating that the features observed in this study reflect typical conditions. Climatological surface nutrients in the spring were depleted except at the front (Fig. 5b in Zhang et al., 2013), coinciding with where we saw Eddies A and B and where nitrate was enhanced (Fig. 2, middle column, fourth row). Climatological chlorophyll was highest at the front (Fig. 5f in Zhang et al., 2013), similar to what was seen in our mean May measurements as well.

July 2019 mean frontal position and structure did not match summer climatological means (Zhang et al., 2011), due to the presence of the shelf water streamer and the Gulf Stream intrusion (Fig. 3 upper right). The offshore deep chlorophyll maxima observed were stronger than in the climatological means (Zhang et al., 2013) due to the influence of Gulf Stream water intrusions. Nitrate measurements and inshore chlorophyll measurements were consistent with climatological mean distributions (Zhang et al., 2013).

Enhancement of diatoms and copepods on the shelf in both May and July 2019 was located within regions of climatological chlorophyll enhancements inshore (Zhang et al., 2013), indicating that our observed abundance of diatom and small copepod may be a typical feature for this region.

5. Conclusion

The MAB shelf-break front is a highly dynamic environment heavily influenced by a variety of forcings, internal and external, both biological and physical. The confluence of these forcings complicates diagnosis of causative mechanisms underlying the observed distributions. In April 2018, chlorophyll enhancement at the front was highly transient, typically lasting on the order of days. Movement of the front obscured this enhancement within Eulerian means, but not when averaging over a frontally-aligned coordinate system. In contrast, enhancement caused by Eddy B in May 2019 was sufficient to affect the mean fields of not only chlorophyll but also diatoms and copepods. These features had a significant effect on mean observations partially due to limited duration of sampling – it is plausible that sampling on scales longer than 2-weeks per cruise may be necessary to isolate upwelling trends within the highly variable frontal environment. However, the involvement of frontal eddies and upstream influences throughout all three cruises highlights the need to consider frontal processes in three dimensions, especially since few of the 23 transect crossings presented herein were free of any features affecting the front itself, such as rings, streamers, intrusions, etc. Though beyond the scope of this paper, all three cruises presented in this study departed from the main transect line to conduct 3-D synoptic sampling, covering in more detail some of the features discussed herein, e.g., the *P. pouchetii* bloom in April 2018 (Smith et al., 2021), the streamer (Zhang et al., 2023) and Gulf Stream intrusions observed in July 2019 (Oliver et al., 2021), and both eddies discussed in May 2019 (Hirzel et al., in prep).

Funding

This research was supported by the National Science Foundation (OCE-1657803, OCE-1658054) and the Dalio Explorer Fund.

Declaration of competing interest

The authors declare that they have no known competing financial interests or personal relationships that could have appeared to influence the work reported in this paper.

Data availability

SPIROPA CTD, DAVPR, and nutrient bottle data are archived at the Biological and Chemical Oceanography Data Management Office (BCO-DMO) project page: https://www.bco-dmo.org/project/748894. VIIRS sea surface temperature and surface chlorophyll imagery are available on the National Aeronautics and Space Administration ocean color page: https://oceancolor.gsfc.nasa.gov/cgi/browse.pl?sen=am.

Acknowledgements

We thank Olga Kosnyrev for data stewardship, our SPIROPA colleagues for overall assistance and support, and the captains, crews, and marine technicians of the *R/V Neil Armstrong, NOAAS Ronald H. Brown*, and *R/V Thomas G Thompson* for their assistance and support at sea. We also thank the OOI program for their operation of the Pioneer Array, which provided valuable context for this study.

Appendix A. Supplementary data

Supplementary data to this article can be found online at https://doi.org/10.1016/j.csr.2023.105113.

References

Archibald, K.M., 2021. The Role of Zooplankton in Regulating Carbon Export and Phytoplankton Community Structure: Integrating Models and Observations. Ph.D. thesis, Massachusetts Institute of Technology, Cambridge MA USA, and Woods Hole Oceanographic Institution, Woods Hole MA USA.

Barth, J., Bogucki, D., Pierce, S., Kosro, P.M., 1998. Secondary circulation associated with a shelfbreak front. Geophys. Res. Lett. 25.

Bandara, K., Varpe, Ø., Wijewardene, L., Tverberg, V., Eiane, K., 2021. Two hundred years of zooplankton vertical migration research. Biol. Rev. 96, 1547–1589.

Benthuysen, J., Thomas, L.N., Lentz, S.J., 2015. Rapid generation of upwelling at a shelf break caused by buoyancy shutdown. J. Phys. Oceanogr. 45, 294–312.

Chapman, D.C., Lentz, S.J., 1994. Trapping of a coastal density front by the bottom boundary layer. J. Phys. Oceanogr. 24, 1464–1479.

Davis, C.S., Hu, Q., Gallager, S., Tang, X., Ashjian, C.J., 2004. Real-time observation of taxa-specific plankton distributions: an optical sampling method. Mar. Ecol.: Prog. Ser. 284, 77–96.

Flagg, C.N., Wallace, D., Kolber, Z., 1997. Cold anticyclonic eddies formed from cold pool water in the southern Middle Atlantic Bight. Continent. Shelf Res. 17 (15), 1839–1867.

Garvine, R.W., Wong, K.-C., Gawarkiewicz, G.G., McCarthy, R.K., 1988. The morphology of shelfbreak eddies. J. Geophys. Res. 93 (C12), 15593–15607.

Gawarkiewicz, G., Chapman, D.C., 1992. The role of stratification in the formation and maintenance of shelf-break fronts. J. Phys. Oceanogr. 22, 753–772.

Gawarkiewicz, G., Bahr, F., Beardsley, R.C., Brink, K.H., 2001. Interaction of a slope eddy with the shelfbreak front in the Middle Atlantic Bight. J. Phys. Oceanogr. 31, 2783–2796.

Gawarkiewicz, G., Brink, K.H., Bahr, F., Beardsley, R.C., Caruso, M., Lynch, J.F., Chiu, C.-S., 2004. A large-amplitude meander of the shelfbreak front during summer south of New England: observations from the Shelfbreak PRIMER experiment. J. Geophys. Res. 109.

Gawarkiewicz, G., Todd, R.E., Zhang, W., Partida, J., Gangopadhyay, A., Monim, M.-U.-H., Fratantoni, P., Malek Mercer, A., Dent, M., 2018. The changing nature of shelf-break exchange revealed by the OOI Pioneer Array. Oceanography 31 (1), 60–70.

Hales, B., Vaillancourt, R., Prieto, L., Marra, J., Houghton, R., Hebert, D., 2009a. High-resolution surveys of the biogeochemistry of the New England shelfbreak front during Summer. J. Mar. Syst. 78, 426–441, 2002.

Hales, B., Hebert, D., Marra, J., 2009b. Turbulent supply of nutrients to phytoplankton at the New England shelf break front. J. Geophys. Res. 114.

Houghton, R.W., Visbeck, M., 1998. Upwelling and convergence in the middle atlantic Bight shelfbreak front. Geophys. Res. Lett. 25, 2765–2768.

Houghton, R.W., Hebert, D., Prater, M., 2006. Circulation and mixing at the New England shelfbreak front: results of purposeful tracer experiments. Prog. Oceanogr. 70, 289–312.
Linder, C.A., Gawarkiewicz, G., 1998. A climatology of the shelfbreak front in the Middle Atlantic Bight. J. Geophys. Res. 103 (18), 423, 405–18.
Loder, J., Shore, J., Hannah, C., Petrie, B.D., 2001. Decadal-scale hydrographic and circulation variability in the Scotia–Maine region. Deep-Sea Res. Pt. II 48, 3–35.
Marra, J., Houghton, R.W., Garside, C., 1990. Phytoplankton growth at the shelf-break front in the middle atlantic Bight. J. Mar. Res. 48, 851–868.
Oliver, H., Zhang, W.G., Smith, W.O., Alatalo, P., Chappell, P.D., Hirzel, A.J., Selden, C. R., Sosik, H.M., Stanley, R.H.R., Zhu, Y., McGillicuddy, D.J., 2021. Diatom hotspots driven by western boundary current instability. Geophys. Res. Lett. 48 (11).
Oliver, H., Zhang, W.G., Archibald, K.M., Hirzel, A.J., Smith, W.O., Sosik, H.M., Stanley, R.H.R., McGillicuddy, D.J., 2022. Ephemeral surface chlorophyll enhancement at the New England shelf break driven by Ekman restratification. J. Geophys. Res. Oceans 127 (1).
O'Reilly, J.E., Bush, D.A., 1984. Phytoplankton primary production on the northwestern Atlantic shelf. Rapp. P.-V. Reun. Cons. Int. Explor. Mer. 183, 255–268.
Pickart, R.S., Torres, D., McKee, T.K., Caruso, M., Przystup, J.E., 1999. Diagnosing a meander of the shelf break current in the Middle Atlantic Bight. J. Geophys. Res. 104.
Pickart, R.S., 2000. Bottom boundary layer structure and detachment in the shelfbreak jet of the Middle Atlantic Bight. J. Phys. Oceanogr. 30 (11), 2668–2686.
Ryan, J.P., Yoder, J.A., Cornillon, P.C., 1999a. Enhanced chlorophyll at the shelfbreak of the mid-atlantic Bight and Georges Bank during the spring transition. Limnol. Oceanogr. 44 (1), 1–11.
Ryan, J.P., Yoder, J.A., Barth, J.A., Cornillon, P.C., 1999b. Chlorophyll enhancement and mixing associated with meanders of the shelf break front in the Mid-Atlantic Bight. J. Geophys. Res. 104 (C10), 23479–23493.
Ryan, J.P., Yoder, J.A., Townsend, D.W., 2001. Influence of a Gulf Stream warm-core ring on water mass and chlorophyll distributions along the southern flank of Georges Bank. Deep-Sea Res. Pt. II 48, 159–178.
Saba, V.S., Hyde, K.J.W., Rebuck, N.D., Friedland, K.D., Hare, J.A., Kahru, M., Fogarty, M.J., 2015. Physical associations to spring phytoplankton biomass interannual variability in the U.S. Northeast Continental Shelf. J. Geophys. Res. Biogeosci. 120, 205–220.
Sherman, K., Jaworski, N.A., Smayda, T.J., 1996. The Northeast Shelf Ecosystem: Assessment, Sustainability and Management. Blackwell Science, Cambridge, Massachusetts, USA.
Smith, W.O., Zhang, W.G., Hirzel, A., Stanley, R.M., Meyer, M.G., Sosik, H., Alatalo, P., Oliver, H., Sandwith, Z., Crockford, E.T., Peacock, E.E., Mehta, A., McGillicuddy, D. J., 2021. A regional, early spring bloom of *Phaeocystis pouchetii* on the New England continental shelf. J. Geophys. Res. Oceans 126 (2).
Wiebe, P.H., Burt, K.H., Boyd, S.H., Morton, A.W., 1976. A multiple opening/closing net and environmental sensing system for sampling zooplankton. J. Mar. Res. 34, 313–326.
Zhang, W.G., Alatalo, P., Crockford, T., Hirzel, A.J., Meyer, M.G., Oliver, H., Peacock, E., Petitpas, C.M., Sandwith, Z., Smith, W.O., Sosik, H.M., Stanley, R.H.R., Stevens, B.L. F., Turner, J.T., McGillicuddy, D.J., 2023. Cross-shelf exchange associated with a shelf-water streamer at the Mid-Atlantic Bight shelf edge. Prog. Oceanogr. 210.
Zhang, W.G., Gawarkiewicz, G.G., McGillicuddy, D.J., Wilkin, J.L., 2011. Climatological mean circulation at the New England shelf break. J. Phys. Oceanogr. 41, 1874–1893.
Zhang, W.G., Gawarkiewicz, G., 2015. Length scale of the finite-amplitude meanders of shelfbreak fronts. J. Phys. Oceanogr. 45, 2598–2620.
Zhang, W.G., McGillicuddy, D.J., Gawarkiewicz, G.G., 2013. Is biological productivity enhanced at the New England shelfbreak front? J. Geophys. Res. Oceans 118, 517–535.